

Estimating heterogeneous wildfire effects using synthetic controls and satellite remote sensing

Feliu Serra-Burriel^{a,b,c}, Pedro Delicado^b, Andrew T. Prata^a, Fernando Cucchietti^a

^aBarcelona Supercomputing Center, Barcelona, Spain

^bDepartment of Statistics and Operations Research, Universitat Politècnica de Catalunya, Barcelona, Spain

^cCorresponding author: feliu.serra@bsc.es

Abstract

Wildfires have become one of the biggest natural hazards for environments worldwide. The effects of wildfires are heterogeneous, meaning that the magnitude of their effects depends on many factors such as geographical region, burn severity, area burned, land management practices, and land cover/vegetation type. Yet, which areas are more affected by these events remains unclear. Here we provide causal evidence of the diverse effects of medium to large wildfires (> 404 hectares) in California throughout a time-span of two decades (1995–2016). We present a novel approach for quantifying and predicting vegetation changes due to wildfires through a time-series analysis of satellite remote sensing data. We also evaluate the method's potential for estimating counterfactual vegetation characteristics for burned regions in order to quantify abrupt system changes. Results show greater changes in Normalised Difference Vegetation Index (NDVI), Normalised Burn Ratio (NBR), and Normalised Difference Moisture Index (NDMI) on regions with lower probability of wildfire incidence. We find that on average, wildfires cause a 25% initial decrease in vegetation health indices (NDVI, NBR and NDMI) after they occur. These effects last for more than a decade post-wildfire, and sometimes change the state of vegetation permanently. We also find that the dynamical effects vary across regions, and have an impact on seasonal cycles of vegetation in later years.

Keywords: Wildfires, Causal inference, Remote Sensing, Synthetic Controls, Landsat

1. Introduction

Wildfires pose a significant natural hazard to society (Paton et al., 2015). Moreover, the increase in the frequency and intensity of extreme weather and climate events lead to an increase in societal vulnerability to wildfires (Easterling et al., 2000; Moritz et al., 2014; Schoennagel et al., 2017). Climate change is expected to increase the amount of areas at risk of large wildfires (Westerling et al., 2011). Given the rise in temperatures, and a future drier climate, as climate projections show (Westerling et al., 2006; Spracklen et al., 2009; Bryant and Westerling, 2014; Schoennagel et al., 2017; Angelo and Du Plessis, 2017), together with changes in the timing of seasons (Westerling, 2016), the situation is expected to worsen (Littell et al., 2018). Wildfires are discrete events with a strong seasonality (National Fire Data Center (U.S.), 2005), but changes in seasons have altered the periodicity and effects of wildfires

(Westerling et al., 2006; Jolly et al., 2015; Westerling, 2016). In order to mitigate the hazards posed by wildfires it is important to quantify post-fire vegetation recovery and loss, allowing for effective short- and long-term land management (Chu and Guo, 2013). Predicting the timeline and capacity for fire-prone regions to return to their pre-fire or an alternative state is also desirable, as post-fire vegetation recovery can lead to a significant carbon sink that can offset carbon losses caused by wildfire events (Hicke et al., 2003; Meng et al., 2018).

Changes in climate occur over decadal timescales. However, the change is constant, and if the change is permanent it may affect the size and frequency of wildfires (Abatzoglou and Williams, 2016; Williams et al., 2019). More specifically, we are studying these events in California, since there is a large amount of freely available data sources for this region, and most of the largest wildfires in recent history in California have occurred since 2017. Moreover, the impacts of wildfires are likely to vary substantially across the state (Bryant and Westerling, 2014). Consequently, the increase of large wildfire frequency and severity necessitates new methods using dynamical models to estimate their effects. The use of remotely sensed time series analysis allows for detecting more subtle changes in ecosystem health and conditions (Li and Banerjee, 2020). Understanding which vegetation is most affected by these events is essential.

Given the complexity of disentangling factors known to influence vegetation and forest composition such as climate-induced changes in meteorology (e.g. wind direction and strength, temperature, and precipitation) and land surface characteristics, long-term, high resolution geospatial datasets are required to estimate or predict the cost of wildfires on vegetation (Dale et al., 2001; Meng et al., 2018; Sturrock et al., 2011; Seidl et al., 2017). Satellite remote sensing has become an invaluable tool for monitoring and assessing wildfire activity (Geist, 2005; Chuvieco, 2012; Meng et al., 2018). In addition, the archive of satellite data suitable for land cover and wildfire assessment spans more than 30 years.

To estimate the effects of wildfires, previous studies have used satellite observations to make comparisons of trends between similar burned and unburned regions (Goetz et al., 2006; Alcaraz-Segura et al., 2010; Bolton et al., 2015). Bright et al. (2019) found that wildfires in temperate forest ecosystems have diverse effects, with some regions taking less than 5 years to more than 13 years to recover pre-wildfire vegetation indices values. However, most of previous analyses did not consider the initial vegetation conditions, nor the differences in climate, as these zones may differ in forest ecosystem, vegetation type or weather. As the natural environment is constantly changing, there can be differences between controls and burned regions in terms of natural gradients such as diversity, fertility and soil moisture (Ibáñez et al., 2019) that need to be accounted for. Previous studies have used differences between pre- and post-wildfires through satellite imagery to compute a post-disturbance regrowth, in both, absolute (growth trend) and relative (recovery indicator) terms (Kennedy et al., 2012). Other studies used control regions as counterfactual vegetation to estimate the decrease in gross primary production (GPP) of terrestrial vegetation after a wildfire (Steiner et al., 2020). Spectral similarities between affected and unaffected

pixels for change detection of ecosystem dynamics on time series have also been explored (Lhermitte et al., 2010). The most detailed methodologies require the combination of remotely sensed and field ground data (Chu and Guo, 2013). However, most of these studies focus on small groups of wildfires that have significant strong impacts on vegetation, with small pre- and post-fire follow-up dynamics. In addition, to our knowledge, no methodology accounts for time-varying confounding factors and the non-stationarity of the vegetation indices time series to estimate the dynamical heterogeneous effects of wildfires. This is an important consideration as decadal increases or decreases in NDVI have been shown to impact analysis of historical wildfire case studies (Hicke et al., 2003). Moreover, these studies are limited by the heterogeneities of the unburned areas used, as they might differ from the heterogeneities in burned regions.

Here we propose a novel approach for estimating the impact of wildfires using the generalised synthetic control (GSC) method (Xu, 2017). The GSC method was developed for estimating the effects of government policies and can be used to measure causal effects from interventions. In this paper we apply the GSC method to long-term (~ 30 years) time-series of satellite-derived vegetation health indices (i.e. NDVI, NDMI, NBR). In particular, we are most interested in the NDVI, as it outperforms other spectral indices' accuracy in areas with heterogeneous vegetation and it is the most robust vegetation index for assessing vegetation recovery (Veraverbeke et al., 2012). Specifically, we consider the surroundings of burned regions to reconstruct the characteristics of vegetation that would have been observed in the absence of a wildfire (referred to hereafter as control areas or control pixels (Veraverbeke et al., 2010)). These regions, as well as the burned areas, are represented as polygons, and the information is aggregated from pixel-level data and averaged to obtain spatial and temporal spectral indices for each of the areas of interest (AOIs). The GSC method also allows us to take into account weather and climate data. As a consequence, we are able to detect decreases in post-fire vegetation seasonal-cycles and estimate vegetation recovery times.

The paper is organised as follows. In Section 2 we provide a description of the study region and satellite data used for our analysis. Section 2 also contains the details of the GSC method and how it was implemented in the present study. Section 3 presents the results of our analysis and in Section 4 we provide a discussion and evaluate the strength of our approach in the context of previous studies. Finally, Section 5 summarises the key findings of our study and outlines avenues for future research.

2. Materials and Methods

2.1. Study Area

The study region considered for the present analysis is the state of California, USA (Fig. 1). The vegetation in this region is predominately classified as shrublands, grasslands, and evergreen forests (Jin et al., 2019). California has a Mediterranean climate, which is characterised by hot and dry summers,

and most of the rainfall is concentrated during the winter period, resulting in high wildfire ignition risk in many areas during the summer months (Bryant and Westerling, 2014).

2.1.1. Burned Areas

From 1996–2016, there were 1054 wildfires with an area larger than 404 hectares in California, out of which, 339 were places that only burned once (Fig. 1). From these 339 wildfires, 22 were prescribed wildfires, 7 were catalogued as unknown source, and 6 were Wildland fire use according to Monitoring Trends in Burn Severity (MTBS) (Eidenshink et al., 2007), that is, natural fires allowed to burn when outlined in a fire management plan and communities are not at risk. The rest of them (304) were catalogued as wildfires and are used in our analysis together with their control areas to define our AOIs (indicated as red and green polygons in Fig. 1). The wildfires span a total area of approximately 5×10^5 hectares. The temporal pattern of wildfire occurrence follows an approximately constant number of wildfires over years, most of these during summer period when fuels are ready to spark, except for a large spike on 2008 with some of the largest wildfires in California’s history. Most of these wildfires occurred in the center and northern non-coastal part of California and in places where the most predominant land cover was shrub/scrub, grassland herbaceous, or evergreen forest.

2.1.2. Control Areas

We generated control areas (or “buffer zones”) around the burned areas (e.g. Controls 1 are the polygons enclosing burned areas from 100m to 1km away from the perimeter of the burned areas, Controls 2 are from 1km to 5km away and Controls 3 are from 5km to 10km away, as shown in Fig. 1), similar to Goetz et al. (2006), used to estimate counterfactual vegetation indices. In addition, we removed any pixels from control regions that intersected neighbouring burned areas overlapping control region boundaries from our analysis, to avoid biasing estimates of counterfactual vegetation.

As we will demonstrate in the next sections, the methodology proposed here shows that the combination of aggregated pixels from control areas together with burned regions is suitable for the estimation of wildfire effects, as the estimation of counterfactual vegetation uses information from all control regions on post-wildfire periods, as well as information from both control and burned regions on pre-wildfire periods. The use of different control regions ensures that the effects are unaltered by potential spillover wildfire effects on the control regions.

2.2. Landsat surface reflectance spectral indices and climate data

Using Landsat Surface Reflectance Derived Spectral Indices (LSR-DSI) time series data (Bolton et al., 2015), extracted with the Google Earth Engine platform (GEE) (Gorelick et al., 2017), we construct NDVI, NDMI and NBR indices for three Landsat satellites (LT5, LT7 and LO8) (Cohen et al., 2017; Roy et al., 2016) masking clouds, shadows and snow pixels with FMASK (Zhu and Woodcock, 2012),

and removing pixels from water bodies such as lakes, reservoirs, rivers and creeks. The Landsat satellites provide a consistent source of 30m per pixel resolution, with a frequency of 16 days. The data was collected using GEE from the beginning of 1990 until the end of 2018. This enables us to obtain a multivariate spatial time series over the regions of interest in the state of California, USA—namely, the regions that burned only once during the observed two-decade period from 1995–2016. We have narrowed down the areas of interest to single-burned regions because we want to estimate causal effects, and the methodology only allows for binary treatment (in the context of this paper, the term *treatment* refers to a wildfire event, and *units* are defined as any particular AOI). The outcome is observed for a longer period (1990-2019), however, these methods require a reasonably long time period before the wildfire occurs, such that the matching of treated and control regions is sufficient. Different pre-fire periods were used considering that at least 3 years are required to capture periodicities and trends, as it is the most elementary cycle of the meteorological element (Han et al., 2011).

Climate data was obtained from the interpolated surface meteorological data GridMET (Abatzoglou, 2013) through GEE as well, to account for precipitation amount (daily total in millimeters), maximum temperature and wind speed (Wind velocity at 10m in m/s) over the desired time period for each area of interest. We use the burning index composed feature from GridMET, which is the National Fire Danger Rating System (NFDRS) fire danger index National Wildfire Coordinating Group (2002), as a proxy for large-wildfire occurrence likelihood, in order to stratify observations by probability of wildfire occurrence and discern different vegetation recovery patterns.

2.3. Statistical analysis

To estimate the heterogeneous effects of wildfires within our study region and time-period, we propose a GSC methodology that uses the Nuclear Norm Matrix Completion Method (NNMCM) (Athey et al., 2018). Analogous to synthetic control methods, the GSC with NNMCM creates synthetic controls for the estimation of vegetation over a region in the absence of a wildfire. This method creates synthetic observations that fit the vegetation dynamics on pre-wildfire periods, and extrapolates it to the post-fire periods, using information from all control regions in post-wildfire time periods. As a result, this allows us to estimate the differences between the observed burned vegetation and the estimated counterfactual vegetation. This methodology also accounts for time-varying factors (such as decadal variations in spectral index) and allows us to approximate the effect of each wildfire separately.

2.3.1. Synthetic Controls

The Generalized Synthetic Control (GSC) method (Xu, 2017) is defined based on the relation between the studied outcome (e.g. NDVI, NBR or NDMI), the observed covariates (e.g. maximum temperature, daily accumulated precipitation, wind speed), and treatments (wildfires) in a functional form. Following

the notation of Xu (2017), let us define Y_{it} as observation i at time t for outcome Y so that

$$Y_{it} = \delta_{it} D_{it} + x_{it}' \beta + \lambda_i' f_t + \epsilon_{it}, \quad (1)$$

where Y_{it} is the observed spectral index of interest, D_{it} is a binary variable indicating whether observation i was burned before time period t , δ_{it} is the estimated effect for observations i at time period t , x_{it}' is a transposed matrix of observed covariates, β is a vector of unknown parameters, f_t is a vector of unobserved common factors, λ_i' is a transposed vector of unknown factor loadings and ϵ_{it} is a matrix containing the error terms.

In order to formalize the notion of causality (Rubin D. B, 1974; Holland, 1986; Rosenbaum and Rubin, 2006), and following the above notation of outcomes on Y_{it} , we define two sets, \mathcal{T} and \mathcal{C} , as the sets in *treatment* and *control* groups respectively. Then, the total number of observations is $N = N_{cr} + N_{tr}$, where N_{tr} is the number of treated observations (areas that burned once), and N_{cr} is the number of untreated observations (control areas that never burned). The time variable t is composed of two parts. The first component, $t \in \{1, 2, \dots, T_0^i\}$, contains the pre-wildfire periods, where T_0^i is the time of the wildfire occurrence for observation i . The second component, $t \in \{T_{0+1}^i, \dots, T_T^i\}$, contains the number of periods observed after the wildfire occurred for each AOI i . We define τ as the minimum number of pre-treatment periods to consider a wildfire, and we collect all observations i that have $t \in \{1^i, \dots, T_0^i\}$, where $T_0^i > \tau$.

We now need to introduce the concept of potential outcome. We define $Y_{it}(1)$ as the outcome observed when units are treated (for $t > T_0^i$), and $Y_{it}(0)$ as the potential outcome, which cannot be observed by definition on treated units. That is, what would have happened in the absence of treatment, or in our case, a wildfire. Next, we shift the observation times for all the units that suffered a wildfire, so that all T_0^i occur at the same time, T_0 . In this way, we formulate the average treatment effect on treated as (Xu, 2017):

$$ATT_{t,t>T_0} = \frac{1}{N_{tr}} \sum_{i \in \mathcal{T}} [Y_{it}(1) - Y_{it}(0)] = \frac{1}{N_{tr}} \sum_{i \in \mathcal{T}} \delta_{it} \quad (2)$$

Hence, our estimate of the treatment effect on treated unit i at time t is given by the difference between the actual observed outcome and its estimated counterfactual \hat{Y}_{it} :

$$\hat{\delta}_{it} = Y_{it}(1) - \hat{Y}_{it}(0). \quad (3)$$

Several assumptions are important for the notion of causality. The first one is that we need to be able to define the relation between vegetation health indices and the observed covariates and treatments in a functional form, as shown above. Second, we need to ensure parallel trends on pre-treatment periods

between treated and untreated units. Third, treatment is considered to be binary. Fourth, we need to assume regularity conditions. Lastly, there is no spatial dependence. That is, we are assuming that treatments are assigned randomly. In order to relax this assumption, we have conditioned on the probability of wildfire to obtain conditional average treatment effects on treated (CATTs). Further discussion on these assumptions can be found in discussion section. The conditional ATT (CATT) is defined as

$$CATT = \mathbb{E}[Y_{it}(1) - Y_{it}(0)|t > T_0, X]$$

where conditional on the value of the observed covariate X , we can infer the expected value of the difference between potential outcomes.

Figure 1 shows that the occurrence of wildfires in California is not spatially homogeneous (Li and Banerjee, 2020), and thus, the probability of different areas burning is unequal. To evaluate CATT in the present study, we propose to condition on the *burn index* obtained from the GridMET interpolated data over the AOIs. That is, we want to estimate the average effect of wildfires on burned regions conditional on the burn index. We segregate groups of observations based on observable characteristics, or clusters of similar probabilities of large wildfire incidence. Wildfires are grouped into 4 different categories using the quartiles of this burning index on pre-wildfire periods. These range from lowest probability of wildfire occurrence to the highest probability of wildfire occurrence. The goal is to find groups of wildfires, such that within those areas, before a wildfire occurs, the probability of a wildfire occurring in any given year is close to being random.

2.3.2. Matrix Completion

The matrix completion method (Athey et al., 2018), develops from the matrix completion literature (Candès and Recht, 2009; Candes and Plan, 2010) a method that allows for the exploitation of both stable patterns over time and stable patterns across units. By means of using the nuclear norm matrix completion estimator, we can obtain estimates of the missing values in the desired outcomes, as well as the estimates of the counterfactual outcomes for each of the treated units, $\hat{Y}_{it}(0)$.

For simplicity, ignoring that we have covariates, what we have is a matrix of observed outcomes (in our case we have the above mentioned spectral indices). Thus, we can model a $N \times T$ matrix of outcomes Y , where N is the number of observations and T is the number of time periods, as:

$$Y = L^* + \epsilon$$

where

$$\mathbb{E}[\epsilon|L^*] = 0$$

with $L^* \in \mathbb{R}^{N \times T}$ and ϵ_{it} is understood as measurement error. Using this technique we can estimate not only the missing values previous to the treatment periods, but also the potential outcomes after the treatment is applied. The use of non-treated observations similar to pre-treatment periods of treated units, as well as information from control regions on post-wildfire periods, allows for accurate estimates of $\hat{Y}_{it}(0)$, calibrating accurately the model on pre- and post-wildfire periods.

Lastly, we define Ω as a set of pairs of indices $(i, t), i \in \{1, \dots, N\}, t \in \{1, \dots, T\}$ of the observed outcomes. One way to formulate the objective function to estimate is as follows:

$$\hat{L} = \arg \min_L \left\{ \frac{1}{|\Omega|} \sum_{(i,t) \in \Omega} (Y_{it} - L_{it})^2 + \lambda_L \|L\|_* \right\}$$

where λ_L is chosen by cross-validation.

3. Results

3.1. Average effect of wildfires

Observing vegetation values from 1990-2019, the average effect of wildfires from 1996-2016 on NDVI was an average initial drop of 25% (Fig. 2) over the absolute value of NDVI, and a slow recovery, with an average negative effect up to 10 years after the event of wildfires (Fig. 2(a), (b)). As we are estimating hypothetical scenarios, our measurement of accuracy is to evaluate the fit on pre-wildfire periods, as well as to visually inspect the hypothetical scenarios. Figure 3 shows the comparison of the fit between control regions vegetation and burned regions vegetation ($R^2 = 0.67$) (a), and the difference between burned regions vegetation and synthetic vegetation estimated on pre-wildfire periods ($R^2 = 0.93$) (b). The Mean Squared Prediction Error (MSPE) for the pre-treatment periods between the counterfactuals estimated and the burned regions is 5 times smaller than the Control region 1 and the burned regions on average. Out of the 304 wildfires studied, only 4 of the areas observed show a larger error of the counterfactual estimated compared to the control regions on pre-wildfire periods. For NBR (Fig. 2 (c), (d)), and NDMI (Fig. 2 (e), (f)), the effect is similar, with NBR showing a larger absolute drop. MSPE on pre-treatment periods is more than 5 times lower than using control regions. Furthermore, in all three ATTs estimated, the δ_{it} on pre-wildfire periods $t < T_0^i$ is approximately 0. The cross validation of λ for the NNMCM was done using the *gsynth* package, (Xu, 2017).

3.2. Stratified effect of wildfires

The results of the synthetic controls reveal the heterogeneous effects of wildfires in different regions. Figure 4 shows that in areas where wildfire occurrence is lower, the effect of the wildfires is greater and persists for longer. It is possible that regions with large NDVI values (e.g. evergreen forests) have lower burning index values because of the weather conditions (e.g. relatively larger humidity). The indices

averages are markedly different for the four groups (see Fig. 4) on pre-wildfire periods, and show different dynamical effects and different recovery patterns after wildfires. All four groups show a drop in spectral index vegetation and moisture following a wildfire event (Fig. 4 (a), (c), (e)). The conditional average effect ($\mathbb{E}(\delta_{it}|X)$) shows that the groups from the lower two quartiles of the burn index (red and blue lines of Fig. 4 (b), (d), (f)) suffer a larger change than the upper two quartiles of the burn index (green and yellow lines Fig. 4(b), (d), (f)). Furthermore, in all four groups, the average effect on pre-wildfire periods is very close to 0 (see Fig. 4 (b), (d) and (e)), similar to Fig. 2. Figures 2 and 4 show that $\hat{\delta}_{it}$ is very close to 0 for all $t < T_0$ – that is, we are fulfilling the parallel trends assumption.

3.3. Cumulative effect of wildfires

Given these long-lasting effects and considering the time period that we are observing, our analysis enables us to not only estimate pre- and post-wildfire differences in spectral indices, but also quantify long-term dynamical changes and compare these. To identify how the effects of wildfires have changed over time, it is instructive to compare subgroups of wildfires across different time-spans (Stevens-Rumann et al., 2018). Specifically, if we divide the whole time-series into two segments (pre- and post-2005), we are able to compare the average cumulative effect $\sum_{it} \delta_{it}$ for up to 10 years post-wildfire (Fig. 5 a, c) of both time periods.

From this analysis, we observe three main differences. First, a larger drop in vegetation is detected in the time span 2006-2016 than in 1995-2005 wildfires. Second, a larger difference between the observed average NDVI and the hypothetical vegetation during recovery is also apparent. Last, a less seasonal-fluctuating vegetation, with a more continuous recovery in vegetation is distinguishable. Figure 5 (b) and (d) also show an increase in the cumulative effect of wildfires ($\sum_{it} \delta_{it}, t > T_0$).

4. Discussion

Our results show similar estimates of time recovery from wildfires (from less than 5 years to more than 13 years for recovery, depending on factors as the region, vegetation or environment, among others (Hicke et al., 2003; Greene et al., 2004; Engel and Abella, 2011)). Although each burned region presents a distinct effect from the abrupt change caused by wildfires, we can effectively quantify the loss from wildfires on vegetation health and moisture indices. The range of effects varies strongly depending on many factors, such as land cover, geographical region and phenology or the interaction of environment and vegetation. Our analysis allows for precise estimates of the effects of wildfires on vegetation through the estimation of counterfactual hypothetical scenarios on the absence of wildfires.

Overall, even though a relatively large amount of pre-wildfire periods are required (~ 5 years) to consider seasonalities and trend changes, we find that this methodology could be extended to other fire-prone regions on Earth, and that this methodology could be potentially used to estimate the effects of other

abrupt changes, always considering the need for control or unaffected regions. The assumptions made to construct the models presented in this study are commonly used in statistical procedures (Xu, 2017), and this methodology is generalizable as the size of our sample and time period studied are sufficient to detect subtle system changes. However, these assumptions could be further validated, for example randomizing treatment with the current data that we have and ensuring that δ_{it} is flat in pre- and post-wildfire periods. For control regions where vegetation is clearly different than the burned regions, counterfactual estimation can be very useful. Hypothetical vegetation for strongly autocorrelated time series with strong seasonalities appear to be harder to model in the long-term. How best to determine when using simpler control regions rather than using synthetic controls is an issue that needs further analysis. In this study, models to estimate average treatment effects from wildfires worked best as there were more pre-wildfire periods to calibrate the synthetic controls, and when there were enough observations post-wildfire. Ultimately, the stratification of meaningful groups shows that this methodology allows for identifying different recovery patterns from different types of vegetation and the interaction of this vegetation with different environments.

4.1. Evidence for changes in wildfire severity and vegetation recovery

The composition of ecosystems has undergone constant change over the previous decades (Dale et al., 2001), and the discrete occurrence of wildfires appears to be increasing (Westerling et al., 2006). These changes are reflected in our data in several ways. First, there is a decrease in overall vegetation on the burned areas, compared to non-burned regions (compare red line with both green lines of Control 1 and Control 2 in Fig. 6). Second, we observe that the time series studied are non-stationary, with an upper trend on the average NDVI of the AOIs burned and non-burned, combined with the increase in aridity, potentially resulting in more fuel and conditions for wildfires to burn. Finally, climate change is affecting fuel flammability in many places, including evergreen forests, and thus, these areas are more prone to burn due to large wildfires (Littell et al., 2009).

Further research needs to be done to understand how changes in climate are affecting vegetation (Rother et al., 2015). These changes will likely also influence the occurrence of extreme weather events in the future (Westerling et al., 2006, 2011; Schoennagel et al., 2017; Abatzoglou and Williams, 2016). The increasing trend on NDVI might be because of sample selection bias, as we are only considering vegetation that burned once, or that did not burn during the time period studied. For many wildfires the long-term effect still remains unclear, but given the size of recent wildfire events, these are expected to be large.

4.2. New vegetation cycle patterns

Figure 7 shows three examples of how diverse effects of wildfires can be. There are areas with vegetation affected by wildfires having permanent shocks, and never returning to previous states of

vegetation, while other areas have recovery periods of less than three years, to more than a decade. This is consistent with previous literature (Hicke et al., 2003; Engel and Abella, 2011), where the impact depends on burn severity, geography, and vegetation. Our analysis enables us to precisely estimate the effects of wildfires.

Wildfires are stochastic events, causing abrupt changes in ecosystems, sometimes resulting in switches to new steady states of vegetation. Figure 7(a) shows the Horse Wildfire in 2005, where vegetation recovered after more than 10 years since the wildfire. The plot also shows how the counterfactual is a better approximation to the observed vegetation than the AOI of Control 1 for this wildfire, as it has been used in previous studies. Figure 7(b) shows the Thurman wildfire, which seems to not have fully recovered from the wildfire after 14 years. The control region is also appropriate, although the synthetic control shows an even better fit on the pre-wildfire periods. Lastly, Figure 7(c) shows a wildfire where we can not know yet if it will recover because we are only observing 5 years after the wildfire. About a fifth of the wildfires studied cannot be fully evaluated yet, as this highly depends on the phenology and the amount of years after wildfires observed are not enough to determine the amount of years the wildfire will take to recover. Although it could be a potential research line for future work, predictions of whether this vegetation will recover or not are out of the scope of this paper.

5. Conclusions

The combination of remote sensing data with quasi-experimental observational techniques such as the GSC method has, as far as we know, not been previously used in environmental studies to compute the causal effects of wildfires on vegetation with synthetic controls. Our results demonstrate that the impact of wildfires on vegetation in California is highly variable depending on several factors (Hicke et al., 2003; Greene et al., 2004; Engel and Abella, 2011). The estimation of counterfactual vegetation, similar to Riaño et al. (2002); Lhermitte et al. (2010), using synthetic controls for larger areas, allows us to observe the effect of each single wildfire, with the help of information collected from the rest of the observations in the same time periods. The nuclear norm matrix completion for synthetic controls method used in this work takes advantage of the information and similarities of observations on pre-wildfire periods, as well as the information from control areas on post-wildfire periods, in order to estimate the effect of wildfires. Hence, the dynamic heterogeneous effects of wildfires can be estimated using Landsat Surface Reflectance - Derived Spectral Indices (LSR-DSI) time-series data. Future lines of study include expanding and comparing potential areas to analyse, study different vegetation phenologies, estimating new indices, and using different satellites or segregation techniques within wildfires.

Our work illustrates the benefit of using control regions to estimate counterfactual vegetation and assess stochastic shocks in vegetation over time. Even for regions with a decrease in vegetation, we can still infer the hypothetical counterfactual scenario of the absence of a wildfire on a burned region.

Considering the probability of wildfire occurrence shows that there are discernible patterns from different wildfires.

This methodology allows us to estimate the heterogeneous dynamic causal effects of large wildfires in accordance with climate change (Abatzoglou and Williams, 2016) and seasonal alteration on vegetation health. The main advantages of this approach are that 1) they improve previous methods using a data-driven methodology for constructing comparable regions to estimate the dynamical wildfire effects; 2) they allow for different times of wildfires or staggered adoption; 3) we monitor vegetation over a large time span, allowing for accurate estimation of the long-term effects of wildfires; 4) we estimate counterfactual spectral indices of vegetation and moisture for each of the observed perimeters; and 5) the observed outcomes, jointly with the proposed method, enable the prediction of counterfactual outcomes for each of the wildfires in question, not only on averages. These models make possible the collection of dynamic estimates of the effects throughout time, with the time granularity observed through satellites. Thus, we can estimate the differences from the effects of wildfires throughout different time periods and the following seasons after wildfires, and observe the changing patterns of vegetation recovery. Our results show that, for some kinds of vegetation and regions, the observed controls surrounding the fires are not a good measurement, whereas synthetic controls are an effective way of measuring what would have happened in the absence of a fire. Wildfire disturbance estimation in this study benefits from the inclusion of control regions that are also affected by climate stress. Our results show that places that were initially less likely to burn, on average, have larger spectral indices values, such as larger NDVI or larger NDMI values, and also suffer a larger nominal drop after the wildfire, meaning that more vegetation might be lost.

There are some major challenges and possible improvements to the methods described here. First, as climate is changing, there is an increasing trend on the size of wildfires. Thus, as the frequency of larger events increases, more areas are being burned more than once. As a result, techniques that include multiple treatments or exposures to wildfires could be considered. Second, burn severity, which combines the direct fire impact and ecosystems responses (Veraverbeke et al., 2010) is heterogeneous within a single wildfire (Bastarrika et al., 2011). Some places are hit harder than others for different reasons (e.g. human land management, vegetation type, etc.). Thus, extending this model to allow for a non-binary or continuous treatment would extend its capabilities to reproduce realistic conditions. In this study we have excluded overlapping wildfires because we wanted to avoid biasing our estimates of counterfactual vegetation. However, studying ways in which we can estimate the effect of a wildfire on vegetation that is recovering from a previous wildfire would further improve this methodology. Third, the segregation of homogeneous comparable treated and untreated AOIs, that are similar on pre-treatment periods is also expected to follow in future research.

This data-driven methodology is a combination of a quasi-experimental setting with remote sensing

data and advanced time series analysis technique for causal inference. Results show that the amount of vegetation lost is increasing, not only because of the increase in the size of wildfires, but also because of the types of vegetation that are being burned. As we want to identify causal effects, we are only considering large wildfire areas that burned once. Moreover, there is an upper trend on NDVI over time over the AOIs. Thus, further studies are required to better understand such abrupt changes in ecosystems as wildfires on vegetation recovery patterns.

The methodology explained in this study could be applied to other fire-prone regions around the world. Using GEE can help further expand this methodology to new regions, allowing to compare wildfire effects over different regions on Earth. The only requirement for this would be to find already available perimeters of large wildfires. Replicating this study over many countries could help identify which areas are hit worse by wildfires across the globe, and which kind of vegetation and phenologies are more severely affected by wildfires. Another possible line of future research would be to expand the data used in this study and use this methodology with other shocks on vegetation, such as plagues or pests. Despite the aforementioned challenges, the results point towards significant opportunities ahead.

6. Acknowledgements

We thank all the people that contributed to this research with insightful discussions and comments, including Fred Prata, Miquel Serra-Burriel, Ana Costa-Ramon, Christian Fons-Rosen, Eduardo Graells-Garrido, Patricio Reyes, as well as Guillermo Marin for the help with figures and Victor Paradis for the help editing. Serra-Burriel would also like to thank the Barcelona Supercomputing Center for the Severo Ochoa Mobility Grant, and Delicado would like to thank the Spanish Ministerio de Ciencia e Innovación for the grant MTM2017-88142-P, and A. T. P. acknowledges funding from the European Union's Horizon 2020 research and innovation programme under the Marie Skłodowska-Curie grant agreement H2020-MSCA-COFUND-2016-754433.

The code used in this study is available at www.github.com/feliuserra/wildfires_effects.

7. Description of author's responsibilities

F. S.-B. led the writing of the paper, produced the figures, downloaded and processed the Landsat data and performed the synthetic controls analysis. P. D. and F. C. contributed to statistical analysis and mathematical formation of the synthetic controls method. A. T. P. contributed to the satellite remote sensing analysis. All authors contributed to the interpretation of results and writing of the manuscript.

References

D. Paton, P. T. Buergelt, F. Tedim, S. McCaffrey, Wildfires, in: Wildfire Hazards, Risks and Disasters, Elsevier, 2015, pp. 1–14. URL: <https://linkinghub.elsevier.com/retrieve/pii/B9780124104341000014>. doi:10.1016/B978-0-12-410434-1.00001-4.

D. R. Easterling, J. L. Evans, P. Y. Groisman, T. R. Karl, K. E. Kunkel, P. Ambenje, Observed variability and trends in extreme climate events: A brief review, *Bulletin of the American Meteorological Society* 81 (2000) 417–425. doi:10.1175/1520-0477(2000)081<0417:OVATIE>2.3.CO;2.

M. A. Moritz, E. Batllori, R. A. Bradstock, A. M. Gill, J. Handmer, P. F. Hessburg, J. Leonard, S. McCaffrey, D. C. Odion, T. Schoennagel, A. D. Syphard, Learning to coexist with wildfire, *Nature* 515 (2014) 58–66. doi:10.1038/nature13946.

T. Schoennagel, J. K. Balch, H. Brenkert-Smith, P. E. Dennison, B. J. Harvey, M. A. Krawchuk, N. Mietkiewicz, P. Morgan, M. A. Moritz, R. Rasker, M. G. Turner, C. Whitlock, Adapt to more wildfire in western North American forests as climate changes, *Proceedings of the National Academy of Sciences of the United States of America* 114 (2017) 4582–4590. doi:10.1073/pnas.1617464114.

A. L. Westerling, B. P. Bryant, H. K. Preisler, T. P. Holmes, H. G. Hidalgo, T. Das, S. R. Shrestha, Climate change and growth scenarios for California wildfire, *Climatic Change* 109 (2011) 445–463. doi:10.1007/s10584-011-0329-9.

A. L. Westerling, H. G. Hidalgo, D. R. Cayan, T. W. Swetnam, Warming and earlier spring increase Western U.S. forest wildfire activity, *Science* 313 (2006) 940–943. doi:10.1126/science.1128834.

D. V. Spracklen, L. J. Mickley, J. A. Logan, R. C. Hudman, R. Yevich, M. D. Flannigan, A. L. Westerling, Impacts of climate change from 2000 to 2050 on wildfire activity and carbonaceous aerosol concentrations in the western United States, *Journal of Geophysical Research* 114 (2009) 1–17. doi:10.1029/2008jd010966.

B. P. Bryant, A. L. Westerling, Scenarios for future wildfire risk in California: Links between changing demography, land use, climate, and wildfire, *Environmetrics* 25 (2014) 454–471. doi:10.1002/env.2280.

M. J. Angelo, A. Du Plessis, Research handbook on climate change and agricultural law, *Research Handbook on Climate Change and Agricultural Law* (2017) 1–472. doi:10.4337/9781784710644.

A. L. R. Westerling, Increasing western US forest wildfire activity: Sensitivity to changes in the timing of spring, *Philosophical Transactions of the Royal Society B: Biological Sciences* 371 (2016). doi:10.1098/rstb.2015.0178.

J. S. Littell, D. McKenzie, H. Y. Wan, S. A. Cushman, Climate Change and Future Wildfire in the Western United States: An Ecological Approach to Nonstationarity, *Earth's Future* 6 (2018) 1097–1111. doi:10.1029/2018EF000878.

National Fire Data Center (U.S.), The seasonal nature of fires, Fema (2005) vi, 19 p. URL: <http://www.usfa.fema.gov/statistics/reports/pubs/seasonal.shtml>.

W. M. Jolly, M. A. Cochrane, P. H. Freeborn, Z. A. Holden, T. J. Brown, G. J. Williamson, D. M. Bowman, Climate-induced variations in global wildfire danger from 1979 to 2013, *Nature Communications* 6 (2015) 1–11. doi:10.1038/ncomms8537.

T. Chu, X. Guo, Remote sensing techniques in monitoring post-fire effects and patterns of forest recovery in boreal forest regions: A review, *Remote Sensing* 6 (2013) 470–520. doi:10.3390/rs6010470.

J. A. Hicke, G. P. Asner, E. S. Kasischke, N. H. French, J. T. Randerson, G. J. Collatz, B. J. Stocks, C. J. Tucker, S. O. Los, C. B. Field, Postfire response of North American boreal forest net primary productivity analyzed with satellite observations, *Global Change Biology* 9 (2003) 1145–1157. doi:10.1046/j.1365-2486.2003.00658.x.

R. Meng, J. Wu, F. Zhao, B. D. Cook, R. P. Hanavan, S. P. Serbin, Measuring short-term post-fire forest recovery across a burn severity gradient in a mixed pine-oak forest using multi-sensor remote sensing techniques, *Remote Sensing of Environment* 210 (2018) 282–296. URL: <https://doi.org/10.1016/j.rse.2018.03.019>. doi:10.1016/j.rse.2018.03.019.

J. T. Abatzoglou, A. P. Williams, Impact of anthropogenic climate change on wildfire across western US forests, *Proceedings of the National Academy of Sciences of the United States of America* 113 (2016) 11770–11775. doi:10.1073/pnas.1607171113.

A. P. Williams, J. T. Abatzoglou, A. Gershunov, J. Guzman-Morales, D. A. Bishop, J. K. Balch, D. P. Lettenmaier, Observed Impacts of Anthropogenic Climate Change on Wildfire in California, *Earth's Future* 7 (2019) 892–910. doi:10.1029/2019EF001210.

S. Li, T. Banerjee, Spatial and temporal patterns of wildfires in California, *Earth and Space Science Open Archive* (2020) 20. URL: <https://doi.org/10.1002/essoar.10504419.1>. doi:10.1002/essoar.10504419.1.

V. H. Dale, L. A. Joyce, S. Mcnulty, R. P. Neilson, M. P. Ayres, M. D. Flannigan, P. J. Hanson, L. C. Irland, A. E. Lugo, C. J. Peterson, D. Simberloff, F. J. Swanson, B. J. Stocks, B. Michael Wotton, Climate Change and Forest Disturbances, *BioScience* 51 (2001) 723. doi:10.1641/0006-3568(2001)051[0723:ccaf]2.0.co;2.

R. N. Sturrock, S. J. Frankel, A. V. Brown, P. E. Hennon, J. T. Kliejunas, K. J. Lewis, J. J. Worrall, A. J. Woods, Climate change and forest diseases, *Plant Pathology* 60 (2011) 133–149. doi:10.1111/j.1365-3059.2010.02406.x.

R. Seidl, D. Thom, M. Kautz, D. Martin-Benito, M. Peltoniemi, G. Vacchiano, J. Wild, D. Ascoli, M. Petr, J. Honkaniemi, M. J. Lexer, V. Trotsiuk, P. Mairota, M. Svoboda, M. Fabrika, T. A. Nagel, C. P. Reyer, Forest disturbances under climate change, *Nature Climate Change* 7 (2017) 395–402. URL: <http://dx.doi.org/10.1038/nclimate3303>. doi:10.1038/nclimate3303.

H. Geist, Our earth's changing land: an encyclopedia of land-use and land-cover change, Greenwood Publishing Group, 2005.

E. Chuvieco, Remote sensing of large wildfires: in the European Mediterranean Basin, Springer Science & Business Media, 2012.

S. J. Goetz, G. J. Fiske, A. G. Bunn, Using satellite time-series data sets to analyze fire disturbance and forest recovery across Canada, *Remote Sensing of Environment* 101 (2006) 352–365. doi:10.1016/j.rse.2006.01.011.

D. Alcaraz-Segura, E. Chuvieco, H. E. Epstein, E. S. Kasischke, A. Trishchenko, Debating the greening vs. browning of the North American boreal forest: Differences between satellite datasets, *Global Change Biology* 16 (2010) 760–770. doi:10.1111/j.1365-2486.2009.01956.x.

D. K. Bolton, N. C. Coops, M. A. Wulder, Characterizing residual structure and forest recovery following high-severity fire in the western boreal of Canada using Landsat time-series and airborne lidar data, *Remote Sensing of Environment* 163 (2015) 48–60. URL: <http://dx.doi.org/10.1016/j.rse.2015.03.004>. doi:10.1016/j.rse.2015.03.004.

B. C. Bright, A. T. Hudak, R. E. Kennedy, J. D. Braaten, A. Henareh Khalyani, Examining post-fire vegetation recovery with Landsat time series analysis in three western North American forest types, *Fire Ecology* 15 (2019). doi:10.1186/s42408-018-0021-9.

I. Ibáñez, K. Acharya, E. Juno, C. Karounos, B. R. Lee, C. McCollum, S. Schaffer-Morrison, J. Tourville, Forest resilience under global environmental change: Do we have the information we need? A systematic review, *PLoS ONE* 14 (2019) 1–17. doi:10.1371/journal.pone.0222207.

R. E. Kennedy, Z. Yang, W. B. Cohen, E. Pfaff, J. Braaten, P. Nelson, Spatial and temporal patterns of forest disturbance and regrowth within the area of the Northwest Forest Plan, *Remote Sensing of Environment* 122 (2012) 117–133. URL: <http://dx.doi.org/10.1016/j.rse.2011.09.024>. doi:10.1016/j.rse.2011.09.024.

J. L. Steiner, S. Robertson, S. Teet, J. Wang, X. Wu, Y. Zhou, D. Brown, X. Xiao, Grassland Wildfires in the Southern Great Plains: Monitoring Ecological Impacts and Recovery, *Remote Sensing* (2020) 1–15.

S. Lhermitte, J. Verbesselt, W. W. Verstraeten, P. Coppin, A pixel based regeneration index using time series similarity and spatial context, *Photogrammetric Engineering and Remote Sensing* 76 (2010) 673–682. doi:10.14358/PERS.76.6.673.

Y. Xu, Generalized synthetic control method: Causal inference with interactive fixed effects models, *Political Analysis* 25 (2017) 57–76. doi:10.1017/pan.2016.2.

S. Veraverbeke, I. Gitas, T. Katagis, A. Polychronaki, B. Somers, R. Goossens, Assessing post-fire vegetation recovery using red-near infrared vegetation indices: Accounting for background and vegetation variability, *ISPRS Journal of Photogrammetry and Remote Sensing* 68 (2012) 28–39. URL: <http://dx.doi.org/10.1016/j.isprsjprs.2011.12.007>. doi:10.1016/j.isprsjprs.2011.12.007.

S. Veraverbeke, S. Lhermitte, W. W. Verstraeten, R. Goossens, The temporal dimension of differenced Normalized Burn Ratio (dNBR) fire/burn severity studies: The case of the large 2007 Peloponnese wildfires in Greece, *Remote Sensing of Environment* 114 (2010) 2548–2563. URL: <http://dx.doi.org/10.1016/j.rse.2010.05.029>. doi:10.1016/j.rse.2010.05.029.

S. Jin, C. Homer, L. Yang, P. Danielson, J. Dewitz, C. Li, Z. Zhu, G. Xian, D. Howard, Overall methodology design for the United States national land cover database 2016 products, *Remote Sensing* 11 (2019). doi:10.3390/rs11242971.

J. Eidenshink, B. Schwind, K. Brewer, Z.-L. Zhu, B. Quayle, S. Howard, A Project for Monitoring Trends in Burn Severity, *Fire Ecology* 3 (2007) 3–21. doi:10.4996/fireecology.0301003.

N. Gorelick, M. Hancher, M. Dixon, S. Ilyushchenko, D. Thau, R. Moore, Google earth engine: Planetary-scale geospatial analysis for everyone, *Remote sensing of Environment* 202 (2017) 18–27.

W. B. Cohen, S. P. Healey, Z. Yang, S. V. Stehman, C. K. Brewer, E. B. Brooks, N. Gorelick, C. Huang, M. J. Hughes, R. E. Kennedy, T. R. Loveland, G. G. Moisen, T. A. Schroeder, J. E. Vogelmann, C. E. Woodcock, L. Yang, Z. Zhu, How Similar Are Forest Disturbance Maps Derived from Different Landsat Time Series Algorithms?, *Forests* 8 (2017) 1–19. doi:10.3390/f8040098.

D. P. Roy, V. Kovalskyy, H. K. Zhang, E. F. Vermote, L. Yan, S. S. Kumar, A. Egorov, Characterization of Landsat-7 to Landsat-8 reflective wavelength and normalized difference vegetation index continuity, *Remote Sensing of Environment* 185 (2016) 57–70. URL: <http://dx.doi.org/10.1016/j.rse.2015.12.024>. doi:10.1016/j.rse.2015.12.024.

Z. Zhu, C. E. Woodcock, Object-based cloud and cloud shadow detection in Landsat imagery, *Remote Sensing of Environment* 118 (2012) 83–94. URL: <http://dx.doi.org/10.1016/j.rse.2011.10.028>. doi:10.1016/j.rse.2011.10.028.

H. Han, M. Ma, P. Yan, Y. Song, Periodicity analysis of NDVI time series and its relationship with climatic factors in the Heihe River Basin in China, *Remote Sensing for Agriculture, Ecosystems, and Hydrology XIII* 8174 (2011) 817429. doi:10.11117/12.897938.

J. T. Abatzoglou, Development of gridded surface meteorological data for ecological applications and modelling, *International Journal of Climatology* 33 (2013) 121–131. doi:10.1002/joc.3413.

U. S. D. o. A. National Wildfire Coordinating Group, *Gaining an Understanding of the National Fire Danger Rating System* (2002).

S. Athey, M. Bayati, N. Doudchenko, G. Imbens, K. Khosravi, Matrix completion methods for causal panel data models, Technical Report, National Bureau of Economic Research, 2018.

Rubin D. B., Estimating causal effects of treatment in randomized and nonrandomized studies, *Journal of Educational Psychology* 66 (1974) 688–701. URL: http://www.fsb.muohio.edu/lij14/420{_}paper{_}Rubin74.pdf.

P. W. Holland, Statistics and causal inference, *Journal of the American statistical Association* 81 (1986) 945–960.

P. R. Rosenbaum, D. B. Rubin, The central role of the propensity score in observational studies for causal effects, *Matched Sampling for Causal Effects* (2006) 170–184. doi:10.1017/CBO9780511810725.016.

E. J. Candès, B. Recht, Exact matrix completion via convex optimization, *Foundations of Computational Mathematics* 9 (2009) 717–772. doi:10.1007/s10208-009-9045-5.

E. J. Candes, Y. Plan, Matrix completion with noise, *Proceedings of the IEEE* 98 (2010) 925–936.

C. S. Stevens-Rumann, K. B. Kemp, P. E. Higuera, B. J. Harvey, M. T. Rother, D. C. Donato, P. Morgan, T. T. Veblen, Evidence for declining forest resilience to wildfires under climate change, *Ecology Letters* 21 (2018) 243–252. doi:10.1111/ele.12889.

D. F. Greene, J. Noël, Y. Bergeron, M. Rousseau, S. Gauthier, Recruitment of *Picea mariana*, *Pinus banksiana*, and *Populus tremuloides* across a burn severity gradient following wildfire in the southern boreal forest of Quebec, *Canadian Journal of Forest Research* 34 (2004) 1845–1857. URL: <https://doi.org/10.1139/x04-059>. doi:10.1139/x04-059.

E. C. Engel, S. R. Abella, Vegetation recovery in a desert landscape after wildfires: Influences of community type, time since fire and contingency effects, *Journal of Applied Ecology* 48 (2011) 1401–1410. doi:10.1111/j.1365-2664.2011.02057.x.

J. S. Littell, D. Mckenzie, D. L. Peterson, A. L. Westerling, Climate and wildfire area burned in western U.S. ecoregions, 1916–2003, *Ecological Applications* 19 (2009) 1003–1021. doi:10.1890/07-1183.1.

M. T. Rother, T. T. Veblen, L. G. Furman, A field experiment informs expected patterns of conifer regeneration after disturbance under changing climate conditions, *Canadian Journal of Forest Research* 45 (2015) 1607–1616. doi:10.1139/cjfr-2015-0033.

D. Riaño, E. Chuvieco, S. Ustin, R. Zomer, P. Dennison, D. Roberts, J. Salas, Assessment of vegetation regeneration after fire through multitemporal analysis of AVIRIS images in the Santa Monica Mountains, *Remote Sensing of Environment* 79 (2002) 60–71. doi:10.1016/S0034-4257(01)00239-5.

A. Bastarrika, E. Chuvieco, M. P. Martín, Mapping burned areas from landsat TM/ETM+ data with a two-phase algorithm: Balancing omission and commission errors, *Remote Sensing of Environment* 115 (2011) 1003–1012. URL: <http://dx.doi.org/10.1016/j.rse.2010.12.005>. doi:10.1016/j.rse.2010.12.005.

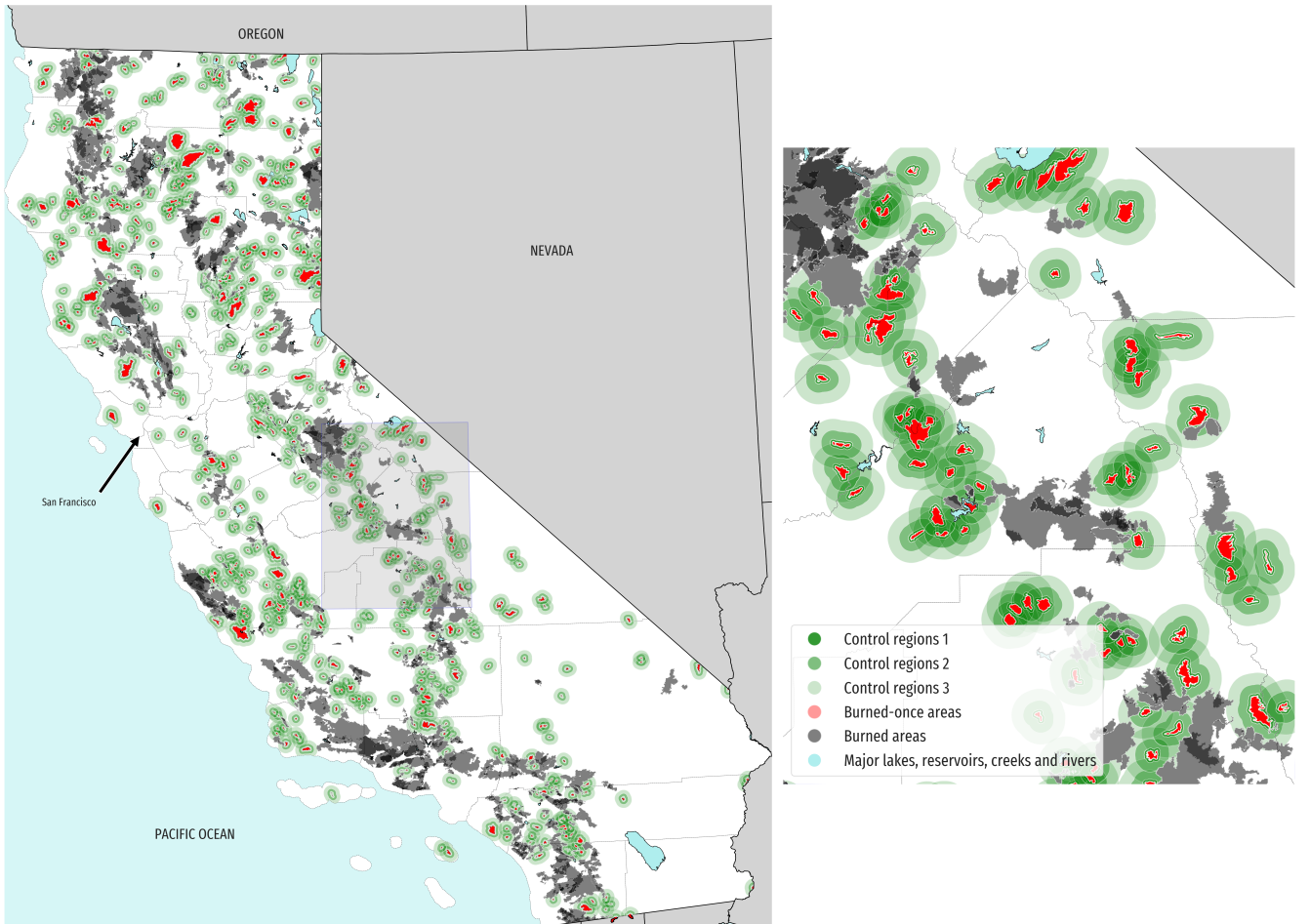


Figure 1: Map of California and the areas of interest. The map shows the regions used in this study. Shown in red are the areas that burned only once during the studied period. In shades of green are shown the three non-overlapping control regions. Gray regions represent areas that suffered from overlapping wildfires, and thus were not included on the estimation of wildfire disturbance effects. Black regions indicate the parts of the areas of the burned perimeters that overlap with more than one wildfire perimeter.

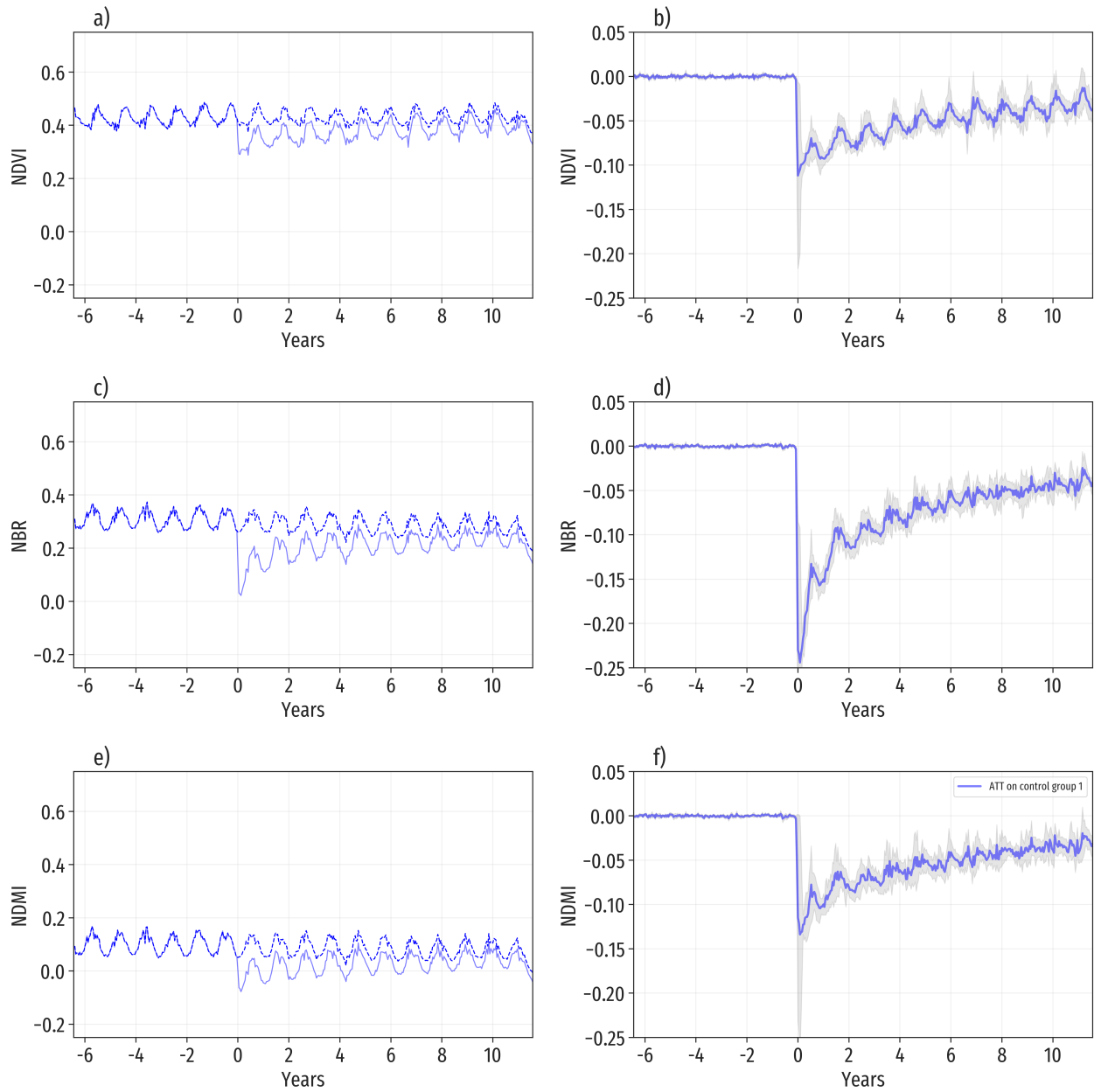


Figure 2: **Average treatment effect of wildfires on Landsat Surface Reflectance Indices (NDVI, NBR and NDMI).** Effect of wildfires on vegetation health and moisture indices. Plots

on the left show the averages observed (light blue), together with their counterfactual estimated (dashed dark blue). On the right, figures show the effect estimated using the NNMCM estimation on vegetation and moisture indices. The light grey bands show the standard errors of the estimated effect for each time period estimated using a bootstrap technique.

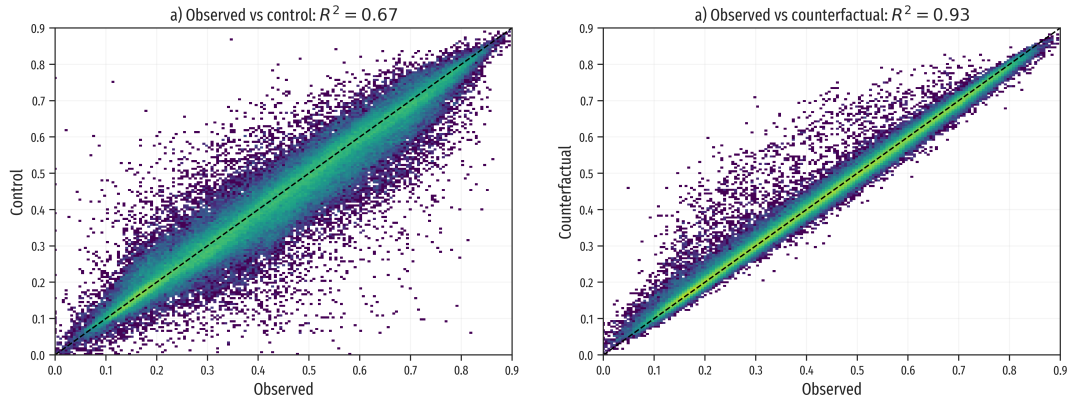


Figure 3: **Error comparison on pre-wildfire periods of controls and synthetic controls.** 2D

Histogram comparison of the 304 wildfires' fit on pre-wildfire periods (with minimum 5 years of pre-wildfire, $\tau = 5$), between observed values and control values (a), and estimated synthetic controls and observed values (b) with a logarithmic color scale. There is an improvement of R^2 going from 0.69 on control regions to 0.93 on counterfactual estimations for pre-wildfire periods. However, the estimated counterfactual vegetation seem to over-estimate actual vegetation for some observations.

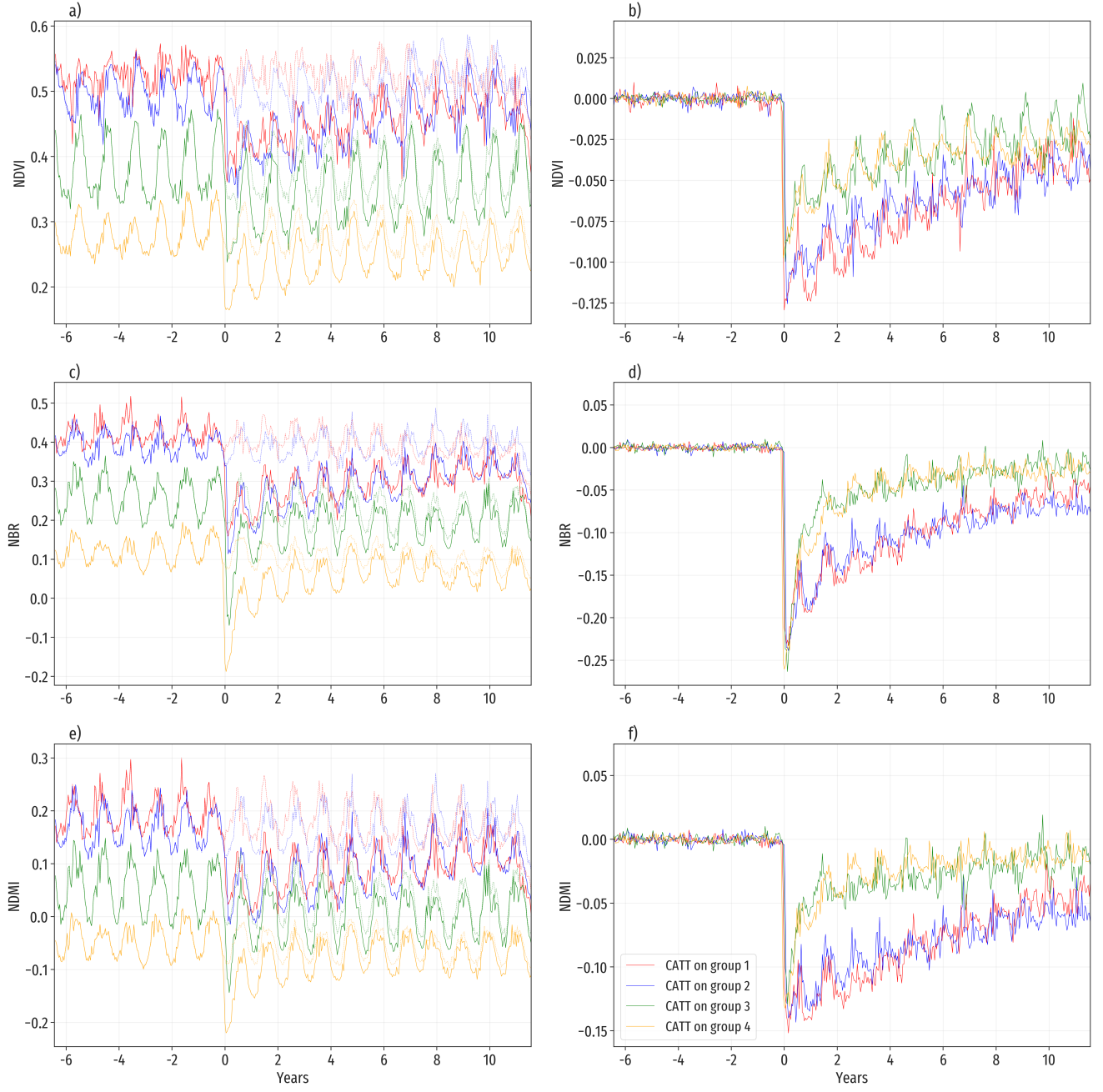


Figure 4: **Average treatment effect of wildfires stratified by probability of wildfire.** Effect of wildfires on different vegetation and moisture indices, stratifying observations with the burning index from GridMET (Abatzoglou, 2013). (a), (c), and (e) show the average NDVI, NBR and NDMI respectively, together with their fitted counterfactual. We observe that on pre-wildfire periods the fit is accurate, and that the hypothetical counterfactual estimation is insightful. (b), (d), and (f) show the average effect from wildfires for each of the different groups of wildfires. Specifically, AOIs within the groups of relatively smaller values of NDVI, NBR and NDMI suffer a smaller drop in nominal terms, and the recovery is faster.

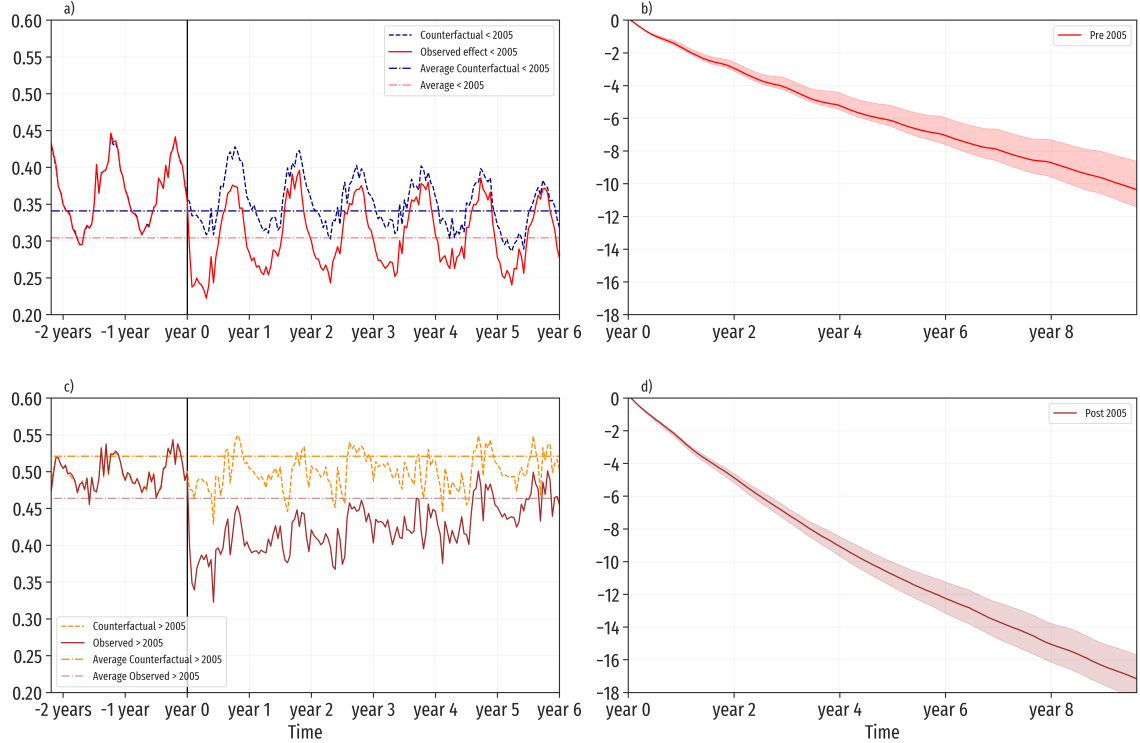


Figure 5: **Cumulative effect comparison of two decades.** Average observed and estimated counterfactual NDVI (a) and cumulative effect on NDVI from wildfires from the period 1995-2005 (b), vs average observed and estimated counterfactual NDVI (c) and cumulative effect on NDVI from wildfires on period 2005-2016 (d). The first decade studied shows a stronger yearly cyclical pattern whereas the second one has larger nominal NDVI values, but less seasonality. The accumulated vegetation loss comparison of the two decades, shows a larger loss for the second period (2005-2016, (d)) than for the first period (1995-2005, (b)).

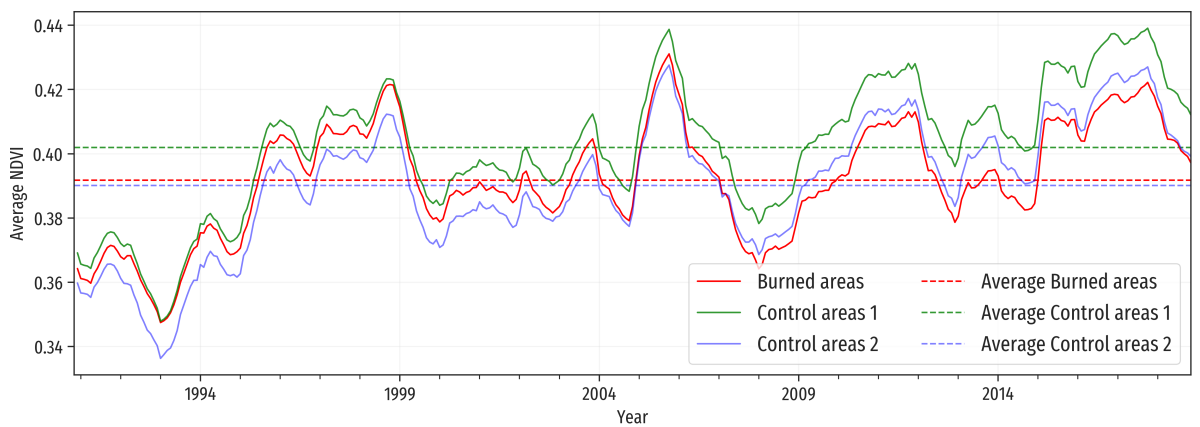


Figure 6: **Average NDVI over aggregated areas of interest over time.** Average NDVI with a rolling mean of one year. Control region 1 refers to the buffer from 100 meters away from the wildfire to 1 km from it and Control region 2 refers to the regions from 1 km to 5 kms away. Control regions do not include regions overlapping other wildfires, as these were excluded.

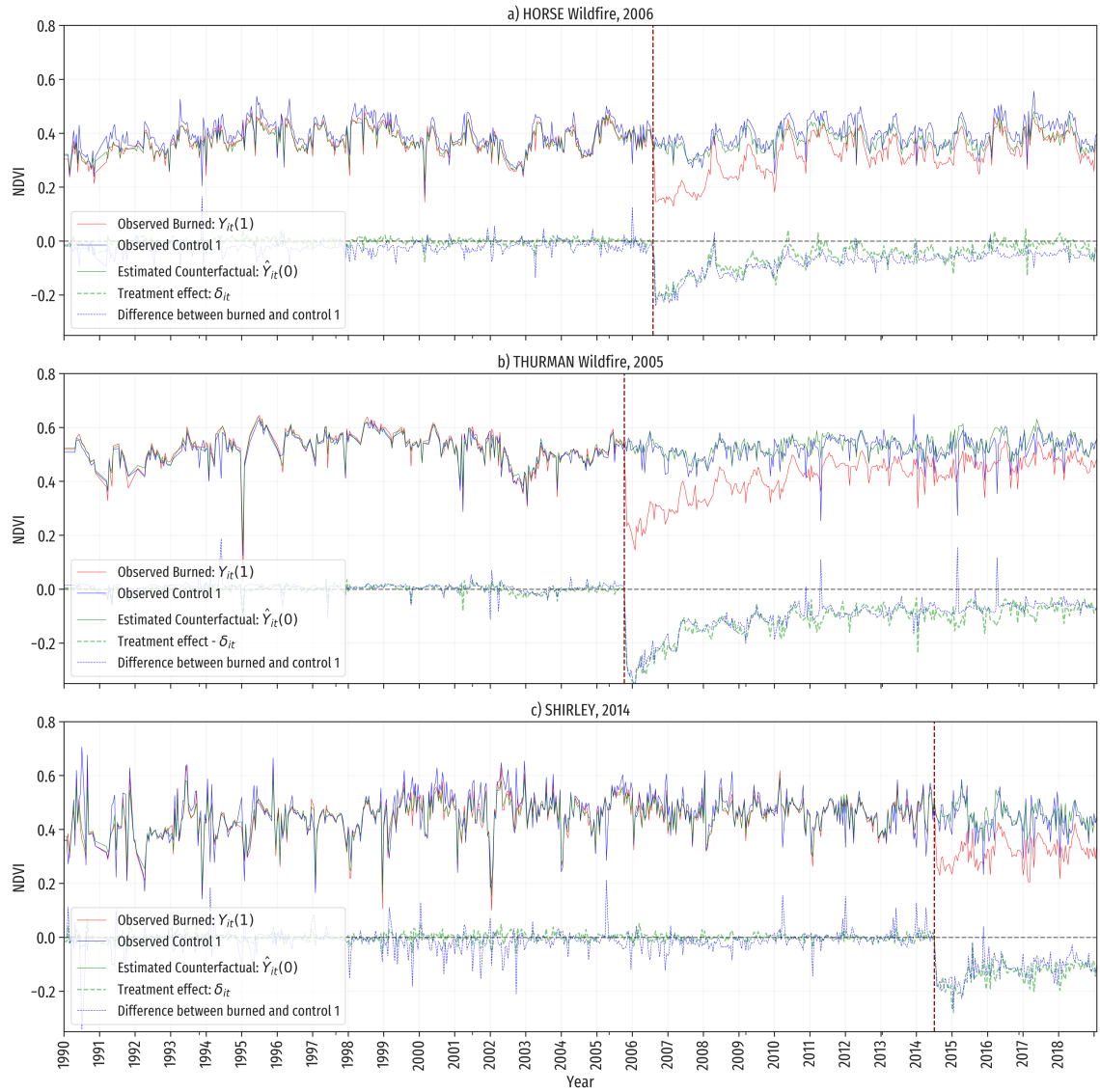


Figure 7: Three sample NDVI time series from areas affected by wildfires, together with their respective control region NDVI time series and counterfactual estimates. (a) Average NDVI over the AOI of wildfire HORSE perimeter, which burned approximately 6766 hectares in 2006. (b) Average NDVI over the AOI of wildfire THURMAN perimeter, which burned approximately 435 hectares in 2005. (c) Average NDVI over the AOI of wildfire SHIRLEY perimeter, which burned approximately 1130 hectares in 2014. Although the three regions had a land cover vegetation predominated by shrubs or scrubs, the effects are different for each wildfire.